Crystallization Behavior of Poly(lactide)/Poly(β-hydroxybutyrate)/Talc Composites

Phuong Nguyen Tri,[1,2] Sandra Domenek,[3] Alain Guinault,[1,4] Cyrille Sollogoub[1,4]

[1]CNAM, P-2AM, 292 rue Saint Martin, 75003 Paris, France

[2]École de Technologie Supérieure, Chaire des Matériaux et Équipements Utilisés en Santé et Sécurité du Travail, 1100 rue Notre-Dame Ouest, Montréal QC, H3C 1K3, Canada

[3]AgroParisTech, UMR 1145 Ingénierie Procédé Aliment, 1 avenue des Olympiades, 91744 Massy, France

[4]Arts et Métiers ParisTech, PIMM, 151, Bd de l'Hôpital, 75013 Paris, France

Correspondence to: C. Sollogoub (E-mail: cyrille.sollogoub@cnam.fr)

ABSTRACT: The morphology and miscibility of commercial poly(lactide) (PLA)/poly(β-hydroxybutyrate) (PHB, from 5 to 20 wt %) blends prepared by melt extrusion method, were investigated using differential scanning calorimetry (DSC) and Fourier transform infrared spectroscopy (FTIR) observations. The results show that for all the studied blend contents, PLA/PHB blends are immiscible. The effects of PHB and talc on the nonisothermal cold crystallization kinetics of PLA were examined using a differential scanning calorimetry (DSC) at different heating rates. PHB acted as a nucleating agent on PLA and the addition of talc to the blend yielded further improvement, since significant increase in the enthalpy peak was observed for samples containing 10 wt % PHB and talc (from 0.5 to 5 phr). The crystallization kinetics were then examined using the Avrami–Jeziorny and Liu–Mo approach. The simultaneous presence of PHB and talc induced a decrease of the crystallization half time. The evolution of activation energies determined with Kissinger's equation suggests that blending with PHB and incorporating talc promote nonisothermal cold crystallization of PLA. The synergistic nucleating effect of PHB and talc was also observed on isothermal crystallization of PLA from the melt. © 2013 Wiley Periodicals, Inc. J. Appl. Polym. Sci. 129: 3355–3365, 2013

INTRODUCTION

Biopolymers have received great attention both in industry and in academia thanks to their advantages of being prepared from renewable resources allowing reducing dependency on fossil resources and being in most cases biodegradable. Poly(lactide) (PLA) is currently one of the most attractive biopolymers being derived from renewable resources, due to its biodegradability and its acceptable mechanical properties.[1,2] However, the main drawbacks of this polymer are its low gas barrier properties, its relative low heat distortion temperature (HDT) and its quite slow crystallization rate.

The low barrier properties of PLA compared to those of synthetic polymers strongly limit its applications in, for instance, food packaging. Different strategies have been used to improve its barrier properties including barrier surface film coating, multilayer coextrusion, plasma deposition, incorporation with nanoclays, or increasing of crystallization degree.[3–6]

Blending of PLA with other biodegradable polymers or conventional synthetic polymers is one of the most effective methods to obtain new properties required for specific end use applications.[7] Generally, polymers having a relative low processing temperature (under 200°C) are suitable for blending with PLA, because PLA undergoes thermal degradation at temperatures above 200°C by hydrolysis, oxidative main chain scission, lactide reformation and inter- or intramolecular transesterification reactions.[8]

Today, PLA has been blended with a variety of polymers, having very different characteristics, biodegradable, or nonbiodegradable, amorphous or semicrystalline, such as polyethylene (PE),[9] polystyrene (PS),[10] polypropylene (PP),[11] polyethylene terephthalate (PET),[12] polyvinyl alcohol (PVA),[13] polycarbonate (PC),[14] polymethyl methacrylate (PMMA),[15] polyethylene oxide (PEO),[16] polysaccharides,[17] poly ε-caprolactone (PCL),[18] polybutylene succinate (PBS),[19] polyethylene glycol (PEG),[20] or different polyhydroxylalkanoates (PHA).[21–23]

Among the PHAs, poly(β-hydroxybutyrate) (PHB) and its copolymers (like poly(β-hydroxybutyrate-*co*-β-hydroxyvalerate) (PHBV) for example) are the most widely studied and commonly used.[24,25] PHB has a similar chemical structure to PLA and is a highly crystalline polymer with high melting point. PLA/PHB binary blends have been extensively studied over the past 20 years, because they can offer property improvements without compromising biodegradability.[26–35]

In particular, many studies have been devoted to the miscibility and compatibility of PLA/PHB blends. Immiscibility between PLA and PHB was widely observed in literature.[27,31,33,34] Data show however that it depended on the molecular weight of both components. Low molecular weight PHB (M_n below $\sim$ 18,000 g mol^{-1}) was found to be miscible with PLLA, while higher molecular weight PHB was not.[26,28] Zhang et al.[32] showed by FTIR spectroscopy potential intermolecular-interactions both in the immiscible and miscible PLLA/PHB blends. Furthermore they found that melt blended samples exhibited greater compatibility than the samples prepared by solvent casting at room temperature due to possible transesterification between PLA and PHB chains.[27] It turns out that, even if high molar mass blends of PLA and PHB are immiscible, the compatibility between the two components depends also on the blend preparation method and composition.

Many investigations have addressed the complex crystallization behavior of this semicrystalline/semicrystalline blend.[26–28,31–35] The crystallization behavior of one component affected by the other was thus thoroughly studied. In particular, Furukawa et al.[31] observed a nucleating effect of PHB in PLA/PHB (80/20) blends yielding smaller cold crystallization times and lower cold crystallization temperatures. Similar results were observed for blends containing low or high molecular weight PHB[34] and finely dispersed PHB crystal particles.[35] The increase of the crystallization rate of PLA has also been achieved using inorganic powders as nucleating agents such as talc or TiO_2,[36–41] and montmorillonite clays.[42,43] Talc, in particular, is an efficient nucleating agent since it can decrease, according to Harris et al.,[38] the half time of crystallization ($t_{1/2}$) of PLA at 115°C from 38.2 min for neat PLA to 0.6 min upon addition of 2 wt % of talc.

The aim of this work is to investigate the combined effect of PHB, blended at low content with PLA, and talc addition on the crystallization behavior and kinetics of PLA. Both nonisothermal cold crystallization and isothermal crystallization from the melt of the PLA/PHB/talc composites are investigated, by using different theoretical kinetic models. While in most of previous studies[26–35] the samples were obtained from solvent casting method, in the present study they are prepared by melt blending technique in a twin screw extruder. This technique presents several interests since it could be really adapted to production process at industrial level and constitutes a solvent-free technique.

EXPERIMENTAL

Materials

PLA 2002D is provided by NatureWorks LLC, containing $\sim$ 4.3 mol % of D-lactide.[44] Molecular weight of PLA samples were determined in our laboratory by using gel permeation chromatography and as follows: number average molecular weight, M_n(PLA) = 100,000 g mol^{-1}, dispersity M_w/M_n = 2.09. This biopolymer has a melt flow index of 5–7 g/10 min (ASTM D1238), and a melting temperature of 160–170°C. Poly(β-hydroxybutyrate) (PHB) is a fine white powder biodegradable polymer supplied by Biomer® (Germany) with number-average molecular weight, M_n (PHB) = 430,000 g mol^{-1}, dispersity M_w/M_n = 1.61. This product has a melting point of 170°C and a glass temperature of 0°C. Talc powder named Luzenac A7C, supplied by RIOTINTO® Minerals, have tapped bulk density of 1.0 g cm^{-3} (ISO 787/11), specific gravity of 2.78 g cm^{-3} (ISO 787/10) and particle median diameter of 2.3 μm (ISO 13317-3).

Fabrication of Composites

PLA pellets and talc powders were dried at 90°C under vacuum during 4 h and PHB was dried during 2 h at the same temperature. The melt blending was carried out at a temperature profile ranging from 180 to 200°C, using a corotating twin screw extruder HAAKE with screw diameter of 16 mm and length to diameter ratio (L/D) 40 : 1. All samples were produced at the same screw speed (200 rpm). The blending ratios of PLA/PHB blends were 95/5, 90/10, and 80/20 by weight. In one of this blend (90/10), the amount of added talc was varied from 0.5 to 5 phr (0.5, 1, 2, and 5 phr) to study non-isothermal and isothermal crystallization kinetics.

Analytical Methods

The molecular weight parameters (number average molecular weight, M_n and dispersity M_w/M_n of PLA and PHB were evaluated on a Shimadzu LC 10 A GPC system equipped with a RIR-10A refractive index detector, an LC-10AD isocratic pump, a DGU-14A degasser, a SIL-10AD automated injector and a CTO-10A thermostat oven. Chloroform (Merck, HPLC grade) was used as eluent with a flow rate of 0.8 mL min^{-1} and with an injection volume of 100 μL at room temperature (25°C). The fractionation was carried out at a series of two PL-Gel mixed C (5 μm, 300 mm) columns and a PL-100A (300 mm) column preceded by a precolumn PL-Gel 5 μm Guard (50 mm). Sample concentrations were 4–5 mg mL^{-1}. Polystyrene of low dispersity (580–1 650 000) was used for calibration.

A DSC apparatus Perkin Elmer, Pyris 1 was used to determine the thermal transitions and the crystallization kinetics of PLA, PLA/PHB blends, and PLA/PHB/talc composites. About 5 mg of the sample were placed in an aluminum crucible of 40 μL. The samples were heated from 0 to 200°C at 10°C min^{-1} and kept for 2 min at 200°C to remove the thermal history. For nonisothermal cold-crystallization study, the samples were then quenched to 0°C at 75°C min^{-1}, and subsequently reheated to 200°C at various heating rates ranging from 5 to 40°C min^{-1}. The endothermic cold crystallization data were then recorded as a function of temperature or time during the second heating. Given enthalpy values are recorded ones, no correction linked to the sample compositions was performed. The instrumental uncertainty of the enthalpy evaluation was evaluated to $\pm$5 J g^{-1}. For isothermal melt crystallization study, the samples were cooled, after removal of the thermal history, at a rate of 20°C

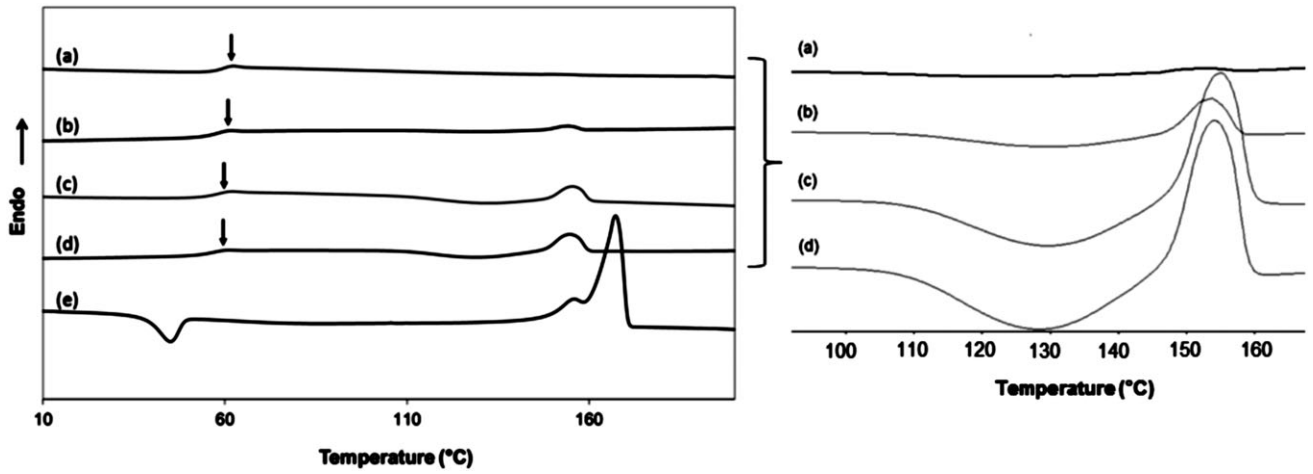

Figure 1. DSC thermograms obtained from the second heating runs with a heating rate of 10°C min^{-1} of neat PLA (a), PLA/PHB (95/5) (b), PLA/PHB (90/10) (c), PLA/PHB (80/20) (d), neat PHB (e), with a zoom around the cold-crystallization peak of PLA.

min^{-1} to one of the several isothermal temperatures (85, 100, 115, and 130°C).

Changes in the structure of PLA and PHB before and after blending were followed by Equinox 55 FTIR spectrometer (Sadis-Bruker Society). Wavelength scanning ranges were taken from 400 to 4000 cm^{-1} with 128 points and at 4 cm^{-1} resolution.

Growth and form of spherulites of neat PLA and its blends film samples during isothermal crystallization process at a fixed temperature were studied using a polarized optical microscope (POM, Leitz Wetzlar), equipped with a digital camera (Leica DC300) and a hot stage (Mettler Toledo PF82HT).

RESULTS AND DISCUSSION

PLA/PHB Blends

Figure 1 displays the DSC curves from the second heating runs at 10°C min^{-1} for neat PLA, neat PHB, and PLA/PHB blends (80/20, 90/10, 95/5 wt %). For these experiments, the cooling rate between the two heating runs was 40°C min^{-1}. Neat PLA exhibits a glass transition around 60°C while fusion peak does not appear clearly. This indicates that PLA does not crystallize much during the DSC cooling and heating processes. On the other hand, neat PHB exhibits a cold crystallization peaks around 45°C, indicating that crystallization during the cooling step is not complete, and a double fusion peak. Following some authors,[31,33] the first fusion peak can be attributed to the fusion of crystals formed during the cooling step, while the second one is associated with the crystals formed from recrystallization during the heating step.

For PLA/PHB blends, since the glass transition temperatures (T_gs) of neat PHB (around 0°C) and neat PLA (around 60°C) are different, the miscibility of the blends can be studied by measuring the T_g of the two components. Because of the low content of PHB in the PLA/PHB blends, the T_g of PHB is difficult to detect, but we clearly see that, when PLA is blended with PHB, T_g of the PLA remains almost unchanged. This suggests that the PLA/PHB blends are immiscible.

It is interesting to note that no cold crystallization peak of PHB is observed in the PLA/PHB blends. Several authors show that PHB inside a blend is crystallizing slower when PHB is the main polymer of the blend[27] or in smaller, more immature crystallites[31]. At low PHB contents (smaller than 20% of PHB) no crystallization is observed.[27,35] In our cases, PHB seems not to be able to crystallize during the cooling run and no peak of cold crystallization of PHB is observed in Figure 1. We observe nevertheless that all PLA/PHB blends exhibit a small cold-crystallization peak and an associated fusion peak, which indicates, in accordance with other authors,[31,34,35] such nucleating effect of the PHB on PLA.

Similar conclusions can be drawn from the Fourier Transform Infrared (FTIR) spectroscopy, a technique very sensitive to structural changes during the crystallization process or transformation of polymeric materials. Figure 2 shows the FTIR spectra of neat PLA, neat PHB and PLA/PHB blends measured from films at room temperature in the region from 700 to 2200 cm^{-1}. We can see in Figure 2 that the PLA and PHB spectra are very similar in the whole analyzed region. This is not a surprise since the chemical structures of PLA and PHB are very close, PHB having only one more (—CH_2—) group in the chain backbone in comparison to PLA. For neat PLA, we observe a fine peak at 1744 cm^{-1}, assigned to amorphous carbonyl stretching of PLA and that remains constant in all the PLA/PHB blends. On the contrary, the absorption peak of PHB at 1719 cm^{-1}, assigned to the crystalline carbonyl stretching of PHB, dominant in neat PHB spectrum, disappears or cannot be clearly detected in the FTIR spectra of the PLA/PHB blends.

In the following study, PLA/PHB (90/10) blend sample was chosen to study the effect of nucleating agent (talc) on the crystallization behavior of PLA. Besides, several theoretical kinetic models have been used to describe the nonisothermal cold-crystallization and isothermal melt-crystallization of neat PLA and PLA/PHB blends with different nucleating agent contents.

PLA/PHB/Talc Composites

Nonisothermal Cold Crystallization Behavior. The study of nonisothermal crystallization has interest because most of industrial

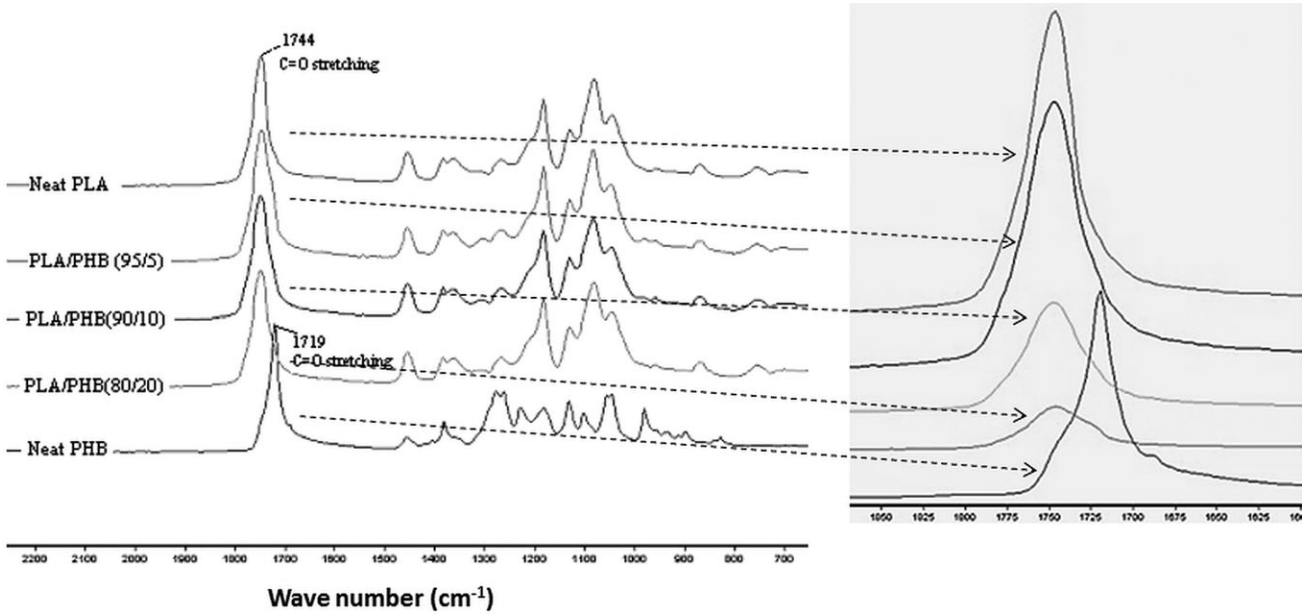

Figure 2. FTIR spectra of neat PLA, neat PHB and PLA/PHB blends.

processes are carried out in nonisothermal conditions (injection moulding, extrusion...). Not fully crystallized PLA could be rearranged at temperatures higher than T_g by cold crystallization. Temperature and rate of cold crystallization are important factors that could determine the end-use applications of polymer materials, especially for polymers whose glass transition temperature is just above ambient temperature like PLA.

For the nonisothermal cold crystallization study, samples have been previously quenched (i.e. cooled at 100°C min^{-1}) after melting. Figure 3 shows the DSC curves of the second heating runs for neat PLA, PLA/PHB blends, and PLA/PHB/talc composites obtained at various heating rates: 5, 10, 20, and 40°C min^{-1}. All the curves, except for the neat PLA, exhibit a cold-crystallization exothermal peak. From these crystallization curves at a given heating rate, we can obtain some useful thermal basic parameters for nonisothermal crystallization as shown Table I: the initial temperature T_{cc} when cold crystallization begins, the crystallization peak temperature T_p, the half time of crystallization which is the time necessary to achieve 50% relative degree of crystallinity ($t_{0.5}$) at temperature of $T_{0.5}$ and the enthalpy of cold crystallization values ΔH_{cc}.

Table I shows that both initial temperature (T_{cc}) and cold crystallization peak temperature (T_p) shift to a higher temperature region, as the heating rates increase. For example, T_{cc} for PLA/PHB (90/10) blend sample is about 28°C higher when the heating rate increases from 5 to 20°C min^{-1}. Besides, we observe that the faster the heating rate, the wider the crystallization peak (Figure 3). At a slower heating rate, there is more time for nucleation within the polymer to be activated, resulting in crystallization at lower temperature. The enthalpy values of cold crystallization (ΔH_{cc}) in Table I show that these values seem to be affected by both the addition of talc and heating histories. In the PLA/PHB blends, it is notable that as the heating rate increases the peaks weaken significantly, suggesting that PLA chains do not have time to self-adjust. PHB, although showing a nucleating effect (Figure 1), seems therefore not to be efficient enough to allow for full crystallization of PLA at faster heating rates and therefore higher peak temperatures.

It appears also from Table I that cold crystallization peak temperature, at a given heating rate, significantly decreases with the increase of talc content (higher than 0.5 phr). It suggests that the presence of PHB and talc promoted cold crystallization of PLA matrix, which is in accordance with previous studies on PLA/PHB blends and PLA/talc composites.[31,34,35,37–40] Still, when the talc content reaches 2 phr, no clear tendencies are observed concerning the evolution of the different temperatures. The sample containing 5 phr talc has a start of crystallization peak almost at the same temperature as the sample at 1 phr. Such a discontinuous behavior was also observed from the melt at a cooling rate of 10°C min^{-1} in the PLA/talc system, but no explanation was given.[40]

The crystallization half time of all the PLA/PHB/talc composites decreased compared to the PLA/PHB blend, and enthalpy values showed that even at the higher heating rates full crystallization of PLA was obtained. For example, in the case of PLA/PHB +5 phr talc at 40°C min^{-1}, the crystallization peak appears at the same temperature as for the PLA/PHB blend at 5°C min^{-1} and the enthalpy of crystallization can be considered as equal, given the instrumental uncertainty. Besides, the decrease in the crystallization half time is significant: from 6.2 to 0.8 min. To investigate more deeply the kinetics of the cold crystallization of the different composites different kinetic models were then used in the following.

Nonisothermal Cold Crystallization Kinetics. The relative degree of crystallinity X_t is a function of temperature and is calculated from the following eq. (1):

$$X_t = \frac{\int_{T_{cc}}^{T_t} (dH_c/dT)/dT}{\int_{T_{cc}}^{T_\infty} (dH_c/dT)/dT} \quad (1)$$

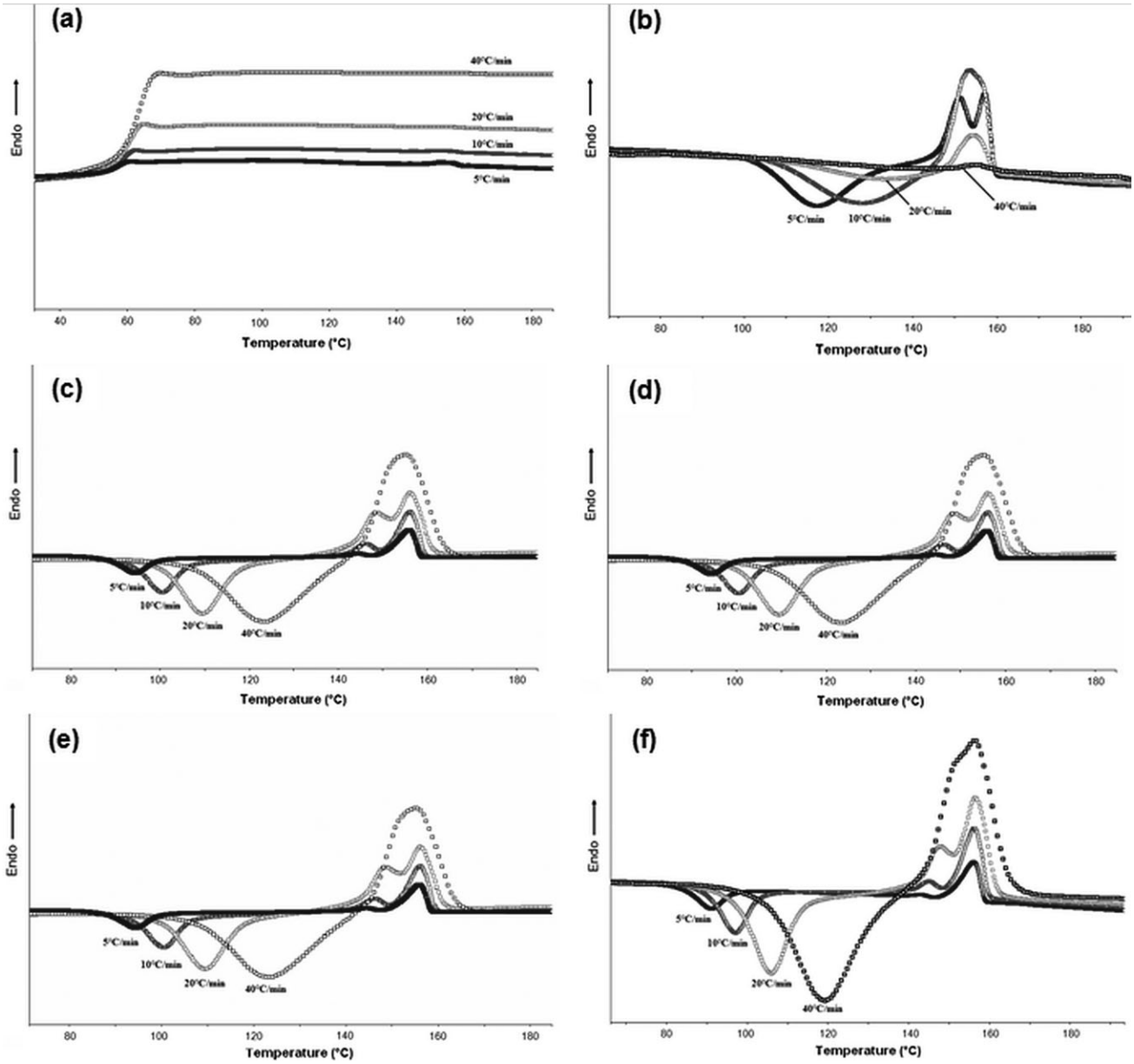

Figure 3. DSC thermograms of nonisothermal cold crystallization process for neat PLA (a), PLA/PHB (90/10) (b), PLA /PHB/talc (90/10/0.5) (c), PLA/PHB/talc (90/10/1) (d), PLA/PHB/talc (90/10/2) (e), PLA/PHB/talc (90/10/5) (f) at different heating rates 5, 10, 20, 40°C min^{-1}.

where T_{cc} is the initial temperature when cold crystallization begins, T_t is the temperature at time t, T_∞ is the temperature in the complete crystalline state, $d\mathrm{H}_c$ is the enthalpy of the crystallization process.

In fact, crystallization temperature values in eq. (3) can be converted into the time scale according to eq. (2) at a given heating rate:

$$t = (T_t - T_{cc})/\lambda \tag{2}$$

where λ is the heating rate.

Figure 4 shows the relative degree of crystallinity (X_t) as a function of time by using eq. (2) on the typical example of the blends PLA/PHB (90/10) [Figure 4(a)] and PLA/PHB/Talc (90/10/5) [Figure 4(b)]. From these curves, we can determine the half time of cold crystallization ($t_{0.5}$) for each sample corresponding to the time at 50% of relative degree of crystallinity. The $t_{0.5}$ values of the different composites investigated are collected in Table I. It appears that the $t_{0.5}$ values of composites decrease as the heating rate increases and the $t_{0.5}$ values decrease with incorporation of talc particles in the formulation, indicating that talc particles accelerate overall crystallization.

Avrami Model. To go further in the study of the crystallization kinetics, different approaches have been carried out on the analysis of the DSC signal. Avrami model[45–47] is widely applied to describe the overall isothermal crystallization, proposing a relation between relative degree of crystallinity (X_t) and elapsed crystallization time t, given in eq. (3):

Table I. Characteristic Parameters for Nonisothermal Cold Crystallization of PLA/PHB (90/10) Blend and PLA/PHB/Talc Composites

Sample	λ (°C min^{-1})	T_{cc} (°C)	$T_{0.5}$ (°C)	T_p (°C)	$t_{0.5}$ (min)	ΔH_{cc} (J g^{-1})
PLA/PHB (90/10)	5	86.3	117.3	117.1	6.2	27.9
	10	98.5	125.7	126.7	2.7	12.7
	20	114.7	132.2	132.7	0.88	1.9
	40	-	-	-	-	-
PLA/PHB/talc (90/10/0.5)	5	86.2	97.2	97.6	2.2	20.2
	10	89.2	103.9	104.2	1.5	24.2
	20	97.2	114.7	114.8	0.9	26.4
	40	103.1	129.9	130.8	0.7	17.6
PLA/PHB/talc (90/10/1)	5	76.5	87.47	88.1	2.2	23.1
	10	79.9	94.5	95.3	1.5	24.5
	20	87.5	102.9	103.1	0.8	27.8
	40	93.6	113.9	113.5	0.5	31.8
PLA/PHB/talc (90/10/2)	5	83.3	94.2	94.5	2.2	17.8
	10	87.8	100.3	100.5	1.3	20.5
	20	95.7	109.5	109.4	0.7	22.3
	40	93.8	123.8	123.5	0.7	28.1
PLA/PHB/talc (90/10/5)	5	76.6	91.1	91.0	2.9	19.6
	10	80.1	96.8	97.2	1.7	21.2
	20	82.7	105.7	106.1	1.2	24.2
	40	87.3	119.1	119.5	0.8	25.6

$$1 - X_t = \exp(-Z_t t^n) \quad (3)$$

where X_t is the relative degree of crystallinity at time t, Z_t is the Avrami rate constant, t is the elapsed crystallization time, n is the Avrami exponent (Avrami index) which characterizes the information about nucleation and growth geometry. Equation (3) converted into logarithmic form is shown below (4):

$$\log[-\ln(1 - X_t)] = \log\ Z_t + n\ \log\ t \quad (4)$$

By using eq. (4), n and Z_t values can be obtained from the slope and the intersection of the curves by plotting log [-ln(1-X_t)] versus log t with the horizontal axis as shown on the basis of the example blends PLA/PHB (90/10) [Figure 4(c)] and PLA/PHB/Talc (90/10/5) [Figure 4(d)]. It is observed that the curves are linear for the PLA/PHB blend at each heating rate studied.

It was noted that in the nonisothermal crystallization process, n and Z_t are not of the same physical nature as in the case of isothermal crystallization because the nonisothermal crystallization temperature constantly varies over time. Considering the nonisothermal character of the process, Jeziorny[48] suggested to include the effect of heating rate (λ) on Z_t. The new crystallization rate constant Z_c is related to the Z_t parameter as shown in eq. (5):

$$\log\ Z_c = (\log\ Z_t)/\lambda \quad (5)$$

Table II presents all n and Z_c values obtained by using equations. (4) and (5) of non-isothermal crystallization for neat PLA/PHB (90/10) and the PLA/PHB/Talc composites under study. Table II indicates that the Z_c values have a tendency to increase with the heating rates and with the talc powders addition whatever the content. For a given heating rate, the Z_c values of composites are higher than those of neat PLA/PHB. These results indicate that the talc microparticles facilitate the cold crystallization of PLA, in agreement with the results of $t_{0.5}$.

For PLA/PHB/talc composites, we observe, at much longer time, a change of slope of the double-log plots, suggesting the appearance of another regime of crystallization and the fact that the mode of spherulitic nucleation and growth is more complex in the composites. This regime can be classically attributed to the occurrence of a secondary crystallization, observed when plasticizer and/or nucleating agent is added in PLA during nonisothermal melt-crystallization by other authors.[39,40]

The average value of the Avrami index value (n) for the PLA/PHB blend is 2.9 while those for composites vary between 3.1 and 3.3, the n values decrease generally with increasing heating rates.

Liu and Mo Approach

Liu et al.[49] proposed a kinetic equation which combines both Avrami and Ozawa model. Ozawa modified Avrami model, considering that the non-isothermal crystallization process is the combination of many infinitely isothermal crystallization processes over crystallization time. This method may be applicable as crystallization occurs at a constant cooling/heating rate. According to the Ozawa theory,[50] the degree of conversion at temperature T, K(T) can be calculated from the following equation:

$$1 - X_t = \exp[-K(T)/\lambda^m] \quad (6)$$

where $K(T)$ is the Ozawa function which depends on crystallization temperature and contains information about the crystallization

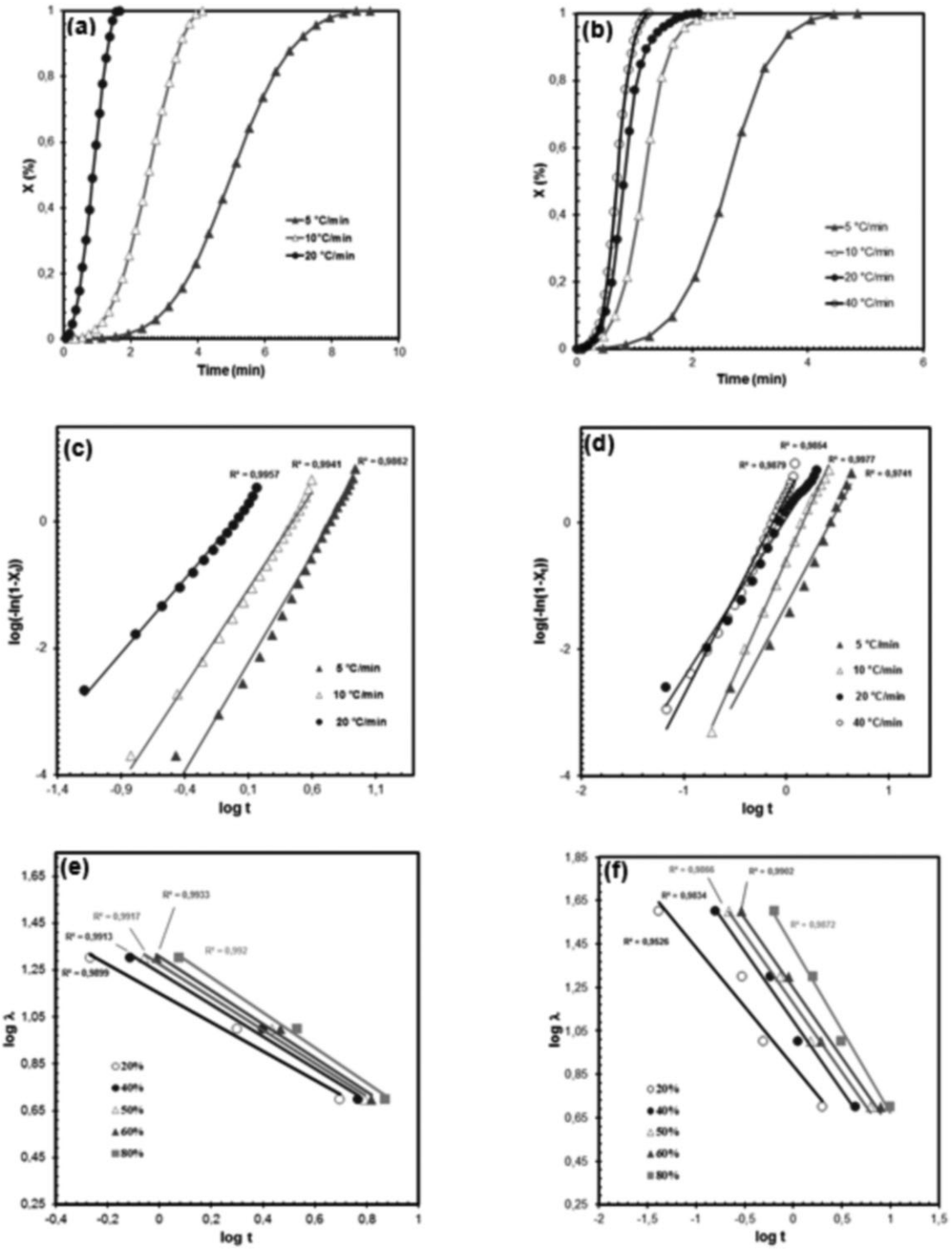

Figure 4. Data analysis of the non-isothermal cold crystallization at different heating rates (5, 10, 20, 40°C min^{-1}) with the help of the modified Avrami and the Liu and Mo model on the examples of PLA/PHB (90/10) (left column) and PLA/PHB/talc (90/10/5) (right column), showing the evolution of relative degree of crystallinity as a function of crystallization time for PLA/PHB (90/10) (a) and PLA/PHB/talc (90/10/5) (b), the plots of log[−ln (1 − X_t)] versus log t for PLA/PHB (90/10) (c) and PLA/PHB/talc (90/10/5) (d), and the plots of log λ versus log t for PLA/PHB (90/10) (e) and PLA/PHB/talc (90/10/5) (f).

process, X_t is the relative degree of crystallinity, λ is the cooling/heating rate (°C min^{-1}) and m is the Ozawa index. Equation (6) may be converted into logarithmic form as eq. (7) below:

$$\log[-\ln(1 - X_t)] = \log\ K(T) - m\ \log\ \lambda \qquad (7)$$

According to Long et al.,[51] with the exception of few polymers (like poly(ethylene terephthalate) and isotactic polypropylene),

Table II. Nonisothermal Cold Crystallization Parameters of PLA/PHB (90/10) Blend and PLA/PHB/Talc Composites Calculated from Avrami Model

Sample	λ (K min^{-1})	n	Z_c	R^2
PLA/PHB (90/10)	5	3.4	0.31	0.9862
	10	3.1	0.73	0.9441
	20	2.3	1.00	0.9957
	–	–	–	–
PLA/PHB/talc (90/10/0.5)	5	3.7	0.52	0.9893
	10	3.3	0.89	0.9893
	20	2.8	1.02	0.9897
	40	3.0	1.39	0.9858
PLA/PHB/talc (90/10/1)	5	3.6	0.54	0.9809
	10	3.3	0.92	0.9644
	20	3.4	1.03	0.9842
	40	2.8	1.04	0.9728
PLA/PHB/talc (90/10/2)	5	3.3	0.56	0.9919
	10	2.7	0.97	0.9838
	20	3.8	1.02	0.9989
	40	2.7	1.02	0.9624
PLA/PHB/talc (90/10/5)	5	3.0	0.55	0.9741
	10	3.6	0.87	0.9977
	20	2.5	1.01	0.9854
	40	3.1	1.02	0.9879

the cooling crystallization of most of the polymeric systems cannot be predicted satisfactorily using the Ozawa model. In particular, for neat PLA, as well as its blends and composites, a deviation from linear Ozawa model was observed.[39,40,52,53] This can be explained by the fact that this model ignores secondary crystallization of the polymer during the nonisothermal crystallization process.

The Liu and Mo approach[49] consists in combining the double logarithmic form of the Avrami and Ozawa model, as shown below (8):

$$\log Z_t + n \log t = \log K(T) - m \log \lambda \tag{8}$$

At a given relative degree of crystallinity X_t, this equation may be rearranged as follows:

$$\log \lambda = \log F(T) - a \log t \tag{9}$$

where $F(T) = [K(T)/Z_t]^{1/m}$ refers to the heating rates value during a crystallization time unit when the system has a well-defined degree of crystallization, a is the ratio of the Avrami index to the Ozawa index, i.e., $a = n/m$, and λ is the heating rate.

According to eq. (9), plotting log λ versus log t at a given relative degree of crystallinity, we can obtain linear curves as shown in Figure 4(e,f) for the example of PLA/PHB (90/10) and PLA/PHB/Talc (90/10/5). The a, F(T) values can be calculated from the slope and interception of these curves with horizontal axis, respectively. The results of these values for PLA/PHB (90/10) and its composites with talc are shown Table III. It appears that the a values are relatively constant, ranging from 0.62 to 0.75 for neat PLA/PHB (90/10) and from 0.54 to 1.77 for PLA/PHB composites. We observe as well that the values F(T) for PLA/PHB composites are systematically higher than those of neat PLA/PHB, except for the last composition with 5 phr of talc. Nevertheless the meaning of these results is questionable and further insight is needed to explain them.

Determination of Activation Energy. The activation energy ΔE (dynamic factor characterizing the process of transport of macromolecular segments to the surface of crystal growth) can be calculated from the crystallization temperature peak (T_p) and the heating rate (λ) using the Kissinger equation:[54]

$$d[\ln(\lambda/T_p^2)] = (-\Delta E/R)d(1/T_p) \tag{10}$$

where R is the universal gas constant. The activation energy values of the nonisothermal cold crystallization of neat PLA/PHB and its composites are easily calculated from the slope of the

Table III. Nonisothermal Cold Crystallization Parameters of PLA/PHB (90/10) Blend and PLA/PHB/Talc Composites Calculated from Liu Approach and Kissinger Method

Sample	X_t (%)	a	$F(T)$	ΔE (kJ mol^{-1})
PLA/PHB (90/10)	20	0.62	13.5	108
	40	0.68	14.9	
	50	0.70	15.5	
	60	0.72	15.9	
	80	0.75	16.8	
PLA/PHB/talc (90/10/0.5)	20	1.55	60.5	70
	40	1.63	69.4	
	50	1.67	73.6	
	60	1.71	77.8	
	80	1.77	86.4	
PLA/PHB/talc (90/10/1)	20	1.37	45.2	89
	40	1.36	44.9	
	50	1.37	45.3	
	60	1.38	46.0	
	80	1.42	49.1	
PLA/PHB/talc (90/10/2)	20	1.51	56.7	79
	40	1.53	59.1	
	50	1.55	60.5	
	60	1.56	61.9	
	80	1.60	65.5	
PLA/PHB/talc (90/10/5)	20	0.54	12.0	79
	40	0.64	14.1	
	50	0.63	13.9	
	60	0.64	14.1	
	80	0.77	17.2	

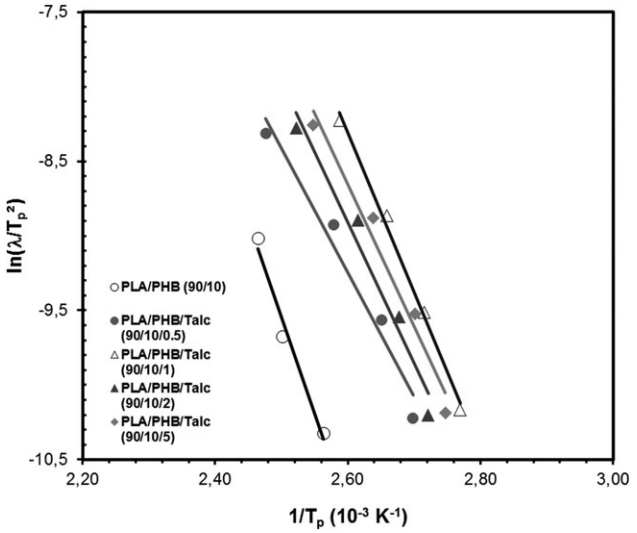

Figure 5. Plots of $\ln(\lambda/T^2_p)$ versus $1/T_p$ during nonisothermal cold crystallization process for PLA/PHB (90/10), PLA/PHB/talc (90/10/0.5), PLA/PHB/talc (90/10/1), PLA/PHB/talc (90/10/2), PLA/PHB/talc (90/10/5).

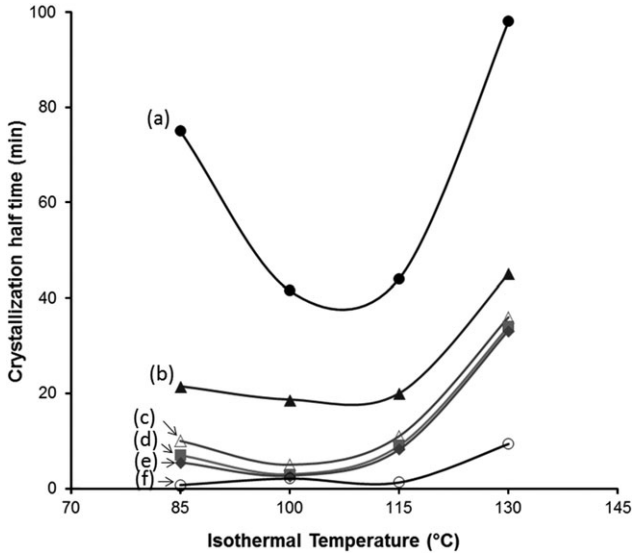

Figure 6. Isothermal-crystallization half time ($t_{0.5}$) for neat PLA (a), PLA/PHB (90/10) (b), PLA/PHB/talc (90/10/0.5) (c), PLA/PHB/talc (90/10/1) (d), PLA/PHB/talc (90/10/5) (e) and neat PHB (f) as a function of isothermal temperature.

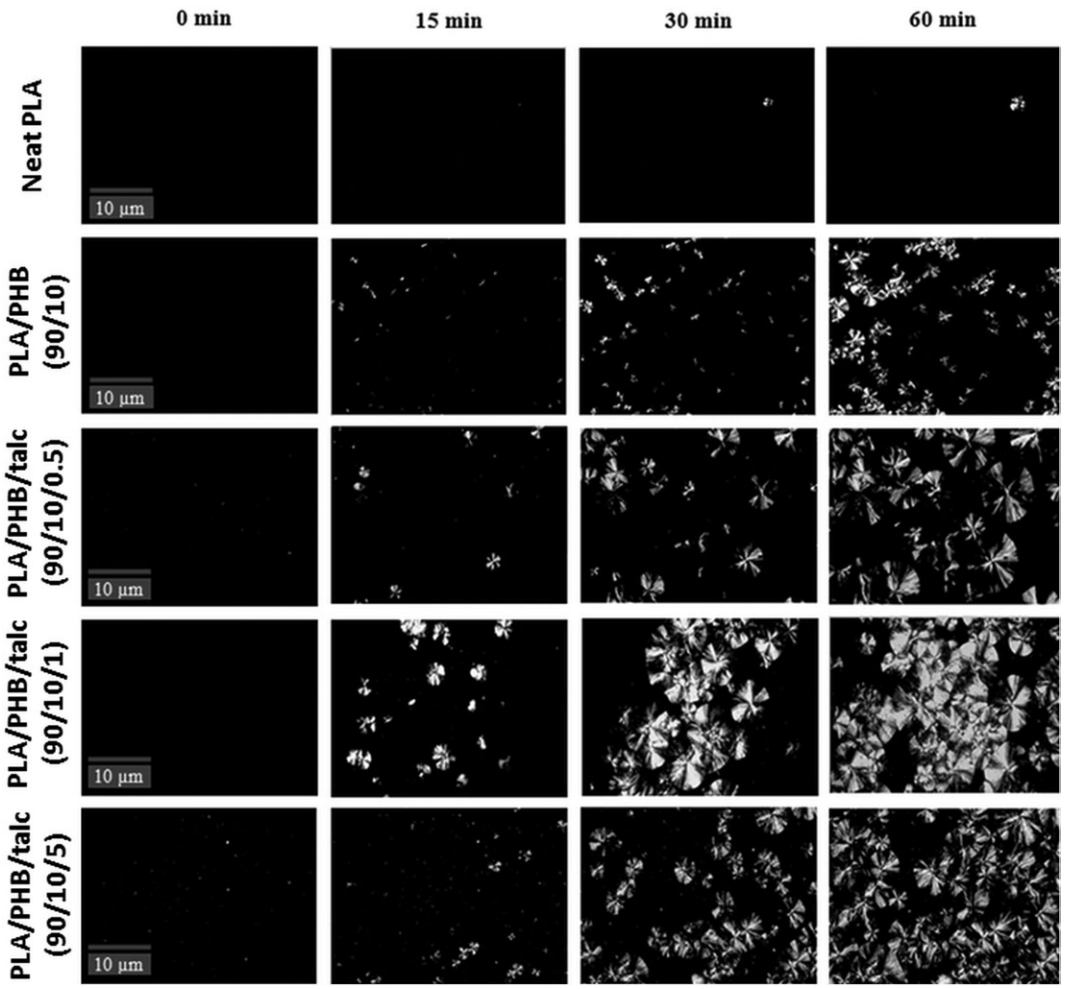

Figure 7. Selected polarization photomicrographs of neat PLA, and composites as a function of isothermal crystallization time at 130°C.

curves plotting ln (λ/T_p^2) versus $1/T_p$, as shown Figure 5. The ΔE values of neat PLA/PHB (90/10) and its composites are given in Table III. We observe that the ΔE values for the composites are markedly lower than those of the neat PLA/PHB matrix due to "nucleating effect" of talc powders.

Isothermal Crystallization Kinetics from the Melt

The addition of nucleating agent into PLA matrix could affect not only the cold crystallization but also the crystallization from the melt. The melt crystallization of PLA, PLA/PHB (90/10) and its composites were investigated in terms of half time of crystallization ($t_{0.5}$) under isothermal conditions at four fixed temperatures ranging from 85 to 130°C.

Figure 6 presents the half time of crystallization ($t_{0.5}$) as a function of isothermal temperature. We can see that the half time curves exhibit a minimum value which is around 110°C for all the samples. This temperature corresponds to the optimum temperature of isothermal crystallization of the samples. Besides, Figure 6 shows that neat PLA has slow crystallization rate and its half time of crystallization values at optimum temperature (108°C) is around 70 min, while neat PHB exhibits the fastest crystallization rate compared to all studied samples. PLA/PHB blend has lower half time crystallization values in comparison with neat PLA, which can be explained by the fact that PHB particles act as "nucleating agent." This effect leads to an increase of the crystallization rates of neat PLA and correlated decrease of the half time of crystallization.[31,34,35]

The addition of 0.5 phr talc effectively decreases the half time of crystallization of PLA/PHB blend to around 6 min. In the presence of 1 phr talc, the minimum of half time crystallization is reduced to about 2.5 min. As regards the effect of the talc content on the half time of crystallization, we can see that using an excess amount of nucleating agent (more than 1 phr) does not have an effective effect on nucleation process. This result can be due to the agglomeration phenomenon of talc microparticles at high level and the limited number of talc particles that could act as nucleating agent to accelerate the nucleation of PLA matrix.

Spherulites growth behavior is investigated using dynamical polarization optical microscopy disposed on a camera that allows observing the morphologies and the development of spherulites during isothermal crystallization. Figure 7 shows the polarized optical photomicrographs of several selected samples taken during the isothermal crystallization at 130°C. It can be observed clearly that the amount of spherulites increases gradually with the isothermal crystallization time. Besides, the crystallization rate increases with the presence of PHB and the addition of talc microparticles. The composites containing talc microparticles have quicker crystallization rate than that of samples without talc microparticles.

CONCLUSIONS

The miscibility and morphology of PLA/PHB blends were investigated by DSC, FTIR, and SEM observations. For all the compositions (5, 10, and 20 wt % of PHB), the blends were found to be immiscible. The PHB particles did not seem to crystallize in the blends and could act as nucleating agent for cold crystallization of PLA.

The combined effect of PHB blending and talc addition on the nonisothermal cold crystallization of PLA was investigated by the use of the theoretical models of Avrami, Jeziorny, Liu, and Mo. Avrami model gave some results that were satisfactory for high relative degree of crystallization. Liu–Mo approach was also used to describe the non-isothermal cold crystallization kinetics. With the presence of PHB and talc, the cold crystallization of PLA significantly increased, as suggested by the increase of the crystallization rate constant.

Isothermal melt crystallization experiments showed that PLA crystallized much faster with PHB and talc addition. At optimum temperature of crystallization (108°C), the half time of isothermal crystallization was reduced from about 70 min for neat PLA to about 2.5 min for PLA/PHB/talc (90/10/1) samples. Incorporating more than 1 phr of talc did not seem beneficial for the crystallization kinetics.

These results can have applicative importance for guiding the optimization of crystallization of PLA, for example during post-annealing processing.

ACKNOWLEDGMENTS

The authors thank Dr. Patrice Lefrançois (CNAM) for SEM observations. They are also grateful to Pr. Jack R. Plimmer USDA, Agricultural Research Service, USA for his discussions during this work.

REFERENCES

1. Drumright, R. E.; Gruber, P. R.; Henton, D. E. *Adv. Mater.* **2000**, *12*, 1841.
2. Gupta, A. P.; Kumar, V. *Eur. Polym. J.* **2007**, *43*, 4053.
3. Gattin, R.; Copinet, A.; Bertrand, C.; Couturier, Y. *Int. Biodet. Biodegrad.* **2002**, *50*, 25.
4. Inagaki, N.; Narushima, K.; Tsutsui, Y.; Ohyama, Y. *J. Adhes. Sci. Technol.* **2002**, *16*, 1041.
5. Rhim, J. W.; Hong, S. I.; Ha, C. S. *LWT Food Sci. Technol.* **2009**, *42*, 612.
6. Colomines, G.; Ducruet, V.; Courgneau, C.; Guinault, A.; Domenek, S. *Polym. Int.* **2010**, *59*, 818.
7. Rasal, R. M.; Janorkar, A. V.; Hirt, D. E. *Prog. Polym. Sci.* **2010**, *35*, 338.
8. Fan, Y.; Nishida, H.; Shirai, Y.; Tokiwa, Y.; Endo, T. *Polym. Degrad. Stab.* **2004**, *86*, 197.
9. Anderson, K. S.; Lim, S. H.; Hillmyer, M. A. *J. Appl. Polym. Sci.* **2003**, *89*, 3757.
10. Mohamed, A.; Gordon, S. H.; Biresaw, G. *J. Appl. Polym. Sci.* **2007**, *106*, 1689.
11. Choudhary, P.; Mohanty, S.; Nayak, S. K. *J. Appl. Polym. Sci.* **2011**, *121*, 3223.
12. Girija, B. G.; Sailaja, R. R. N.; Madras, G. *Polym. Degrad. Stab.* **2005**, *90*, 147.
13. Shuai, X.; He, Y.; Asakawa, N.; Inoue, Y. *J. Appl. Polym. Sci.* **2001**, *81*, 762.

14. Hashima, K.; Nishitsuji, S.; Inoue, T. *Polymer* **2010**, *51*, 3934.
15. Li, S. H.; Woo, E. M. *Polym. Int.* **2008**, *57*, 1242.
16. Nijenhuis, A. J.; Colstee, E.; Grijpma, D. W.; Pennings, A. J. *Polymer* **1996**, *37*, 5849.
17. Zhang, J. F.; Sun, X. S. *Biomacromolecules* **2004**, *5*, 1446.
18. Wu, D.; Zhang, Y.; Yuan, L.; Zhang, M.; Zhou, W. *J. Polym. Sci. B Polym. Phys.* **2010**, *48*, 756.
19. Park, J. W.; Im, S. S. *J. Appl. Polym. Sci.* **2002**, *86*, 647.
20. Hu, Y.; Hu, Y. S.; Topolkaraev, V.; Hiltner, A.; Baer, E. *Polymer* **2003**, *44*, 5681.
21. Takagi, Y.; Yasuda, R.; Yamaoka, M.; Yamane, T. *J. Appl. Polym. Sci.* **2004**, *93*, 2363.
22. Noda, I.; Satkowski, M. M.; Dowrey, A. E.; Marcott, C. *Macromol. Biosci.* **2004**, *4*, 269.
23. Boufarguine, M.; Guinault, A.; Miquelard-Garnier, G.; Sollogoub, C. *Macromol. Mater. Eng.* **2012**, Published online: DOI: 10.1002/mame.201200285.
24. Khanna, S.; Srivastava, A. K. *Process. Biochem.* **2005**, *40*, 607.
25. Savenkova, L.; Gercberga, Z.; Nikolaeva, V.; Dzene, A.; Bibers, I.; Kalnin, M. *Process. Biochem.* **2000**, *35*, 573.
26. Blümm, E.; Owen, A. J. *Polymer* **1995**, *36*, 4077.
27. Zhang, L.; Xiong, C.; Deng, X. *Polymer* **1996**, *37*, 235.
28. Koyama, N.; Doi, Y. *Polymer* **1997**, *38*, 1589.
29. Ohkoshi, I.; Abe, H.; Doi, Y. *Polymer* **2000**, *41*, 5985.
30. Gazzano, M.; Focarete, M. L.; Riekel, C.; Scandola, M. *Biomacromolecules* **2004**, *5*, 553.
31. Furukuwa, T.; Sato, H.; Murakami, R.; Zhang, J.; Duan, Y. X.; Noda, I.; Ochiai, S.; Ozaki, Y. *Macromolecules* **2005**, *38*, 6445.
32. Zhang, J.; Sato, H.; Furukawa, T.; Tsuji, H.; Noda, I.; Ozaki, Y. *J. Phys. Chem. B* **2006**, *110*, 24463.
33. Furukawa, T.; Sato, H.; Murakami, R.; Zhang, J.; Noda, I.; Ochiai, S.; Ozaki, Y. *Polymer* **2007**, *48*, 1749.
34. Hu, Y.; Sato, H.; Zhang, J.; Noda, I.; Ozak, I. Y. *Polymer* **2008**, *49*, 4204.
35. Zhang, M.; Thomas, N. L. *Adv. Polym. Technol.* **2011**, *30*, 67.
36. Buzarovska, A.; Grozdanov, A. *J. Appl. Polym. Sci.* **2012**, *123*, 2187.
37. Li, H. B.; Huneault, M. A. *Polymer* **2007**, *48*, 6855.
38. Harris, A. M.; Lee, E. C. *J. Appl. Polym.* **2008**, *107*, 2246.
39. Xiao, H. W.; Yang, L.; Ren, X.; Jiang, T.; Yeh, J. T. *Polym. Compos.* **2010**, *31*, 2057.
40. Courgneau, C.; Ducruet, V.; Averous, L.; Grenet, J.; Domenek, S. *Polym. Eng. Sci.* **2012**, Published online: DOI: 10.1002/pen.23357.
41. Courgneau, C.; Domenek, S.; Lebossé, R.; Guinault, A.; Avérous, L.; Ducruet, V. *Polym. Int.* **2012**, *61*, 180.
42. Krikorian, V.; Pochan, D. J. *Chem. Mater.* **2003**, *15*, 4317.
43. Nam, J. Y.; Ray, S. S.; Okamoto, M. *Macromolecules* **2003**, *36*, 7126.
44. Li, Y.; Wu, H.; Wang, Y.; Liu, L.; Han, L.; Wu, J.; Xiang, F. *J. Polym. Sci. B Polym. Phys.* **2010**, *48*, 520.
45. Avrami, M. *J. Chem. Phys.* **1939**, *7*, 1103.
46. Avrami, M. *J. Chem. Phys.* **1940**, *8*, 212.
47. Avrami, M. *J. Chem. Phys.* **1941**, *9*, 177.
48. Jeziorny, A. *Polymer* **1978**, *19*, 1142.
49. Liu, T. X.; Mo, Z. S.; Wang, S. E.; Zhang, H. F. *Polym. Eng. Sci.* **1997**, *37*, 568.
50. Ozawa, T. *Polymer* **1971**, *12*, 150.
51. Long, Y.; Shanks, R. A.; Stachurski, Z. H. *Prog. Polym. Sci.* **1995**, *20*, 651.
52. Liu, Y.; Wang, L.; He, Y.; Fan, Z.; Li, S. *Polym. Int.* **2010**, *59*, 1616.
53. Li, M.; Hu, D.; Wang, Y.; Shen, C. *Polym. Eng. Sci.* **2010**, *50*, 2298.
54. Kissinger, H. E. *J. Res. Nat. Bur. Stand.* **1956**, *57*, 217.